Electronic Supplementary Information

# Assembly of Metal Organic Frameworks Based on 4-connected 3,3',5,5'-Azobenzenetetracarboxylic Acid: Structures, Magnetic Properties, and Sensing $Fe^{3+}$ ions

**Min Di, Jingwen Shen, Zheng Cui, Xiaoying Zhang,* and Jingping Zhang***

Advanced Energy Materials Research Center
Faculty of Chemistry, Northeast Normal University
Changchun 130024, P. R. China
† E-mail: zhangxy218@nenu.edu.cn; jpzhang@nenu.edu.cn.

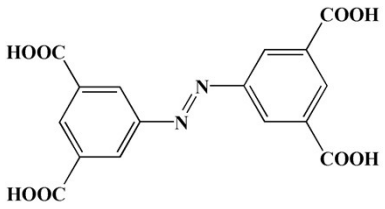


**$H_4$abtc**

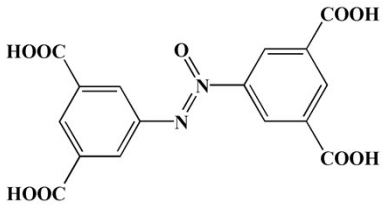


**$H_4$aobtc**

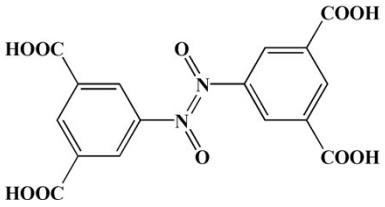


**$H_4$ao$_2$btc**

**Scheme S1** The structure of $H_4$abtc and its two oxidized forms.

**Table S1.** Selected bond distances (Å) and bond angles (°) for complex **1**.

| | | | | | |
|---|---|---|---|---|---|
| Co(1)-O(1) | 2.118(6) | Co(1)-O(10) | 2.074(6) | Co(2)-O(5)#1 | 2.015(5) |
| Co(1)-O(3) | 2.057(5) | Co(1)-O(11) | 2.109(7) | Co(2)-O(6) | 2.339(6) |
| Co(1)-O(4)#1 | 2.030(6) | Co(2)-O(1) | 2.135(5) | Co(2)-O(7)#2 | 2.052(5) |
| Co(1)-O(9) | 2.095(7) | Co(2)-O(2) | 2.005(5) | Co(2)-O(8)#2 | 2.339(6) |
| O(3)-Co(1)-O(1) | | 92.5(2) | O(1)-Co(2)-O(6) | | 58.50(19) |
| O(3)-Co(1)-O(9) | | 89.3(3) | O(1)-Co(2)-O(8)#2 | | 93.0(2) |
| O(3)-Co(1)-O(10) | | 173.5(3) | O(2)-Co(2)-O(1) | | 104.5(2) |
| O(3)-Co(1)-O(11) | | 83.9(3) | O(2)-Co(2)-O(5)#1 | | 97.2(3) |
| O(4)#1-Co(1)-O(1) | | 89.2(2) | O(2)-Co(2)-O(6) | | 92.1(3) |
| O(4)#1-Co(1)-O(3) | | 95.0(3) | O(2)-Co(2)-O(7)#2 | | 98.5(2) |
| O(4)#1-Co(1)-O(9) | | 174.9(3) | O(2)-Co(2)-O(8)#2 | | 158.21(19) |
| O(4)#1-Co(1)-O(10) | | 86.3(3) | O(5)#1-Co(2)-O(1) | | 102.0(2) |
| O(4)#1-Co(1)-O(11) | | 91.2(3) | O(5)#1-Co(2)-O(6) | | 160.1(2) |
| O(9)-Co(1)-O(1) | | 93.3(3) | O(5)#1-Co(2)-O(7)#2 | | 103.7(2) |
| O(9)-Co(1)-O(11) | | 86.6(3) | O(5)#1-Co(2)-O(8)#2 | | 91.6(2) |
| O(10)-Co(1)-O(1) | | 93.8(2) | O(6)-Co(2)-O(8)#2 | | 86.0(2) |
| O(10)-Co(1)-O(9) | | 89.1(3) | O(7)#2-Co(2)-O(1) | | 142.7(2) |
| O(10)-Co(1)-O(11) | | 89.8(3) | O(7)#2-Co(2)-O(6) | | 92.1(2) |
| O(11)-Co(1)-O(1) | | 176.4(2) | O(7)#2-Co(2)-O(8)#2 | | 59.9(2) |

Symmetry transformations used to generate equivalent atoms:

#1 = x+1/2,-y+3/2,-z+5/4 #2 = x+1/2,-y+5/2,-z+5/4

**Table S2.** Selected bond distances (Å) and bond angles (°) for complex **2**.

| | | | | | |
|---|---|---|---|---|---|
| Mn(1)-O(1) | 2.17(4) | Mn(1)-O(2) | 2.1070(8) | Mn(1)-O(3) | 2.148(5) |
| Mn(1)-O(1W) | 2.35(4) | Mn(1)-O(4)#1 | 2.164(4) | Mn(1)-O(5)#2 | 2.172(4) |
| Mn(1)-O(6)#3 | 2.175(4) | Mn(2)-O(7) | 2.24(2) | | |
| O(2)-Mn(1)-O(1) | | 178.1(9) | O(2)-Mn(1)-O(1W) | | 170.6(8) |
| O(2)-Mn(1)-O(3) | | 87.6(2) | O(2)-Mn(1)-O(4)#1 | | 94.66(17) |
| O(2)-Mn(1)-O(5)#2 | | 94.22(17) | O(2)-Mn(1)-O(6)#3 | | 88.5(13) |
| O(1)-Mn(1)-O(3) | | 94.3(9) | O(1)-Mn(1)- O(4)#1 | | 85.5(13) |
| O(1)-Mn(1)-O(5)#2 | | 85.7(13) | O(1)-Mn(1)-O(6) #3 | | 89.6(9) |
| O(3)-Mn(1)-O(1W) | | 101.3(9) | O(3)-Mn(1)- O(4)#1 | | 87.5(2) |
| O(3)-Mn(1)-O(5)#2 | | 90.1(2) | O(3)-Mn(1)- O(6)#3 | | 176.07(19) |
| O(4)#1-Mn(1)-O(1W) | | 88.9(12) | O(4)#1-Mn(1)- O(5)#2 | | 170.71(16) |
| O(4)#1-Mn(1)- O(5)#2 | | 92.63(19) | O(5)#2-Mn(1)-O(1W) | | 82.7(12) |
| O(5)#2-Mn(1)- O(6)#3 | | 90.34(18) | O(6)#3-Mn(1)- O(1W) | | 82.6(9) |

Symmetry transformations used to generate equivalent atoms:

#1 = 1-z, x, 1-y #2 = 3/2-x, 3/2-z, y-1/2 #3 = 3/2-y, 3/2-x, z-1/2

**Table S3.** Selected bond distances (Å) and bond angles (°) for complex **3**.

| | | | | | |
|---|---|---|---|---|---|
| Zn(1)-Zn(2) | 3.0030(13) | Zn(2)-O(3) | 2.009(9) | Zn(3)-O(7) | 1.98(3) |
| Zn(1)-O(1) | 2.046(8) | Zn(2)-O(9)#1 | 2.002(9) | Zn(3)-O(10)#4 | 2.017(7) |
| Zn(1)-O(4) | 2.035(7) | Zn(2)-O(12)#2 | 1.999(9) | Zn(3)-O(11)#5 | 2.017(7) |
| Zn(1)-O(8)#1 | 2.052(7) | Zn(2)-O(13) | 1.939(8) | Zn(3)-O(6A) | 2.06(2) |
| Zn(1)-O(14)#2 | 2.011(8) | Zn(3)-Zn(3)#3 | 3.0058(17) | Zn(3)-O(5A)#3 | 1.942(18) |
| Zn(1)-O(15) | 2.003(6) | Zn(3)-O(5)#3 | 2.06(3) | Zn(3)-O(7A) | 1.999(19) |
| Zn(2)-O(2) | 2.025(10) | Zn(3)-O(6) | 1.986(19) | | |
| O(1)-Zn(1)-Zn(2) | | 74.4(2) | O(2)-Zn(2)-Zn(1) | | 83.6(2) |
| O(1)-Zn(1)-O(8)#1 | | 85.9(4) | O(3)-Zn(2)-Zn(1) | | 75.2(3) |
| O(4)-Zn(1)-Zn(2) | | 83.9(2) | O(3)-Zn(2)-O(2) | | 158.4(4) |
| O(4)-Zn(1)-O(1) | | 158.1(3) | O(9)#1-Zn(2)-Zn(1) | | 87.2(2) |
| O(4)-Zn(1)-O(8)#1 | | 89.8(3) | O(9)#1-Zn(2)-O(2) | | 86.5(5) |
| O(8)#1-Zn(1)-Zn(2) | | 70.8(2) | O(9)#1-Zn(2)-O(3) | | 88.4(4) |
| O(14)#2-Zn(1)-Zn(2) | | 86.8(2) | O(12)#2-Zn(2)-Zn(1) | | 70.8(2) |
| O(14)#2-Zn(1)-O(1) | | 89.3(4) | O(12)#2-Zn(2)-O(2) | | 90.1(5) |
| O(14)#2-Zn(1)-O(4) | | 86.6(4) | O(12)#2-Zn(2)-O(3) | | 86.8(4) |
| O(14)#2-Zn(1)-O(8)#1 | | 157.6(3) | O(12)#2-Zn(2)-O(9)#1 | | 157.9(3) |

| | | | |
|---|---|---|---|
| O(15)-Zn(1)-Zn(2) | 166.4(2) | O(13)-Zn(2)-Zn(1) | 167.2(3) |
| O(15)-Zn(1)-O(1) | 99.2(3) | O(13)-Zn(2)-O(2) | 103.7(4) |
| O(15)-Zn(1)-O(4) | 102.6(3) | O(13)-Zn(2)-O(3) | 97.9(4) |
| O(15)-Zn(1)-O(8)#1 | 97.1(3) | O(13)-Zn(2)-O(9)#1 | 103.5(4) |
| O(15)-Zn(1)-O(14)#2 | 105.3(3) | O(13)-Zn(2)-O(12)#2 | 98.5(4) |
| O(5)#3-Zn(3)-Zn(3)#3 | 76.2(7) | O(11)#5-Zn(3)-O(5)#3 | 156.3(8) |
| O(6)-Zn(3)-Zn(3)#3 | 81.7(6) | O(11)#5-Zn(3)-O(10)#4 | 89.9(4) |
| O(6)-Zn(3)-O(5)#3 | 89.7(12) | O(11)#5-Zn(3)-O(6A) | 88.5(9) |
| O(6)-Zn(3)-O(10)#4 | 161.4(6) | O(6A)-Zn(3)-O(5)#3 | 84.7(13) |
| O(6)-Zn(3)-O(11)#5 | 89.3(7) | O(5A)#3-Zn(3)-O(5)#3 | 12.7(10) |
| O(7)-Zn(3)-Zn(3)#3 | 169.1(9) | O(5A)#3-Zn(3)-O(10)#4 | 88.1(7) |
| O(7)-Zn(3)-O(5)#3 | 100.5(11) | O(5A)#3-Zn(3)-O(11)#5 | 168.9(6) |
| O(7)-Zn(3)-O(6) | 87.9(11) | O(5A)#3-Zn(3)-O(6A) | 87.3(11) |
| O(7)-Zn(3)-O(10)#4 | 110.3(10) | O(5A)#3-Zn(3)-O(7A) | 104.2(8) |
| O(7)-Zn(3)-O(11)#5 | 103.1(9) | O(7A)-Zn(3)-O(5)#3 | 116.2(9) |
| O(10)#4-Zn(3)-Zn(3)#3 | 79.9(3) | O(7A)-Zn(3)-O(10)#4 | 92.4(8) |
| O(10)#4-Zn(3)-O(5)#3 | 83.7(10) | O(7A)-Zn(3)-O(11)#5 | 86.8(6) |
| O(10)#4-Zn(3)-O(6A) | 147.1(6) | O(7A)-Zn(3)-O(6A) | 120.3(10) |
| O(11)#5-Zn(3)-Zn(3)#3 | 80.2(3) | | |

Symmetry transformations used to generate equivalent atoms:

#1 -x+y,-x,z #2 -x+y+1,-x+1,z #3 -x,-x+y,-z+1

#4 x-y,-y+1,-z+1 #5 -x+y,-x+1,z

**Table S4.** Bond valence sum calculations for complex **1**.

| Atom | $Co^{II}$ | $Co^{III}$ |
|---|---|---|
| Co1 | 2.107 | 2.152 |
| Co2 | 1.874 | 1.916 |

**Table S5.** Bond valence sum calculations for complex **2**.

| Atom | $Mn^{II}$ | $Mn^{III}$ |
|---|---|---|
| Mn1 | 2.235 | 2.062 |
| Mn2 | 1.778 | 1.640 |

## Explanations of Crystal Structure Determination

Complex **1**: PLAT910_ALERT_3_B Missing # of FCF Reflection(s) Below Theta (Min).
**Explanation**: Some reflections with high intensities, which made the detector overflow were automatically omitted by the diffractometer. So some reflections were missing.

Complex **3**: PLAT341_ALERT_3_B Low Bond Precision on C-C Bonds
**Explanation**: The quality of crystal was not so good and the data were collected under low temperature. Therefore thermal vibration of the C atoms was so high that the precision of the C-C bonds is low.

PLAT420_ALERT_2_B D-H Without Acceptor O7 – H7AA
PLAT420_ALERT_2_B D-H Without Acceptor O7 – H7AB
PLAT420_ALERT_2_B D-H Without Acceptor O7 – H7A
PLAT420_ALERT_2_B D-H Without Acceptor O7 – H7B
PLAT420_ALERT_2_B D-H Without Acceptor O13 – H13A
PLAT420_ALERT_2_B D-H Without Acceptor O13 – H13B
PLAT420_ALERT_2_B D-H Without Acceptor O15 – H15B

**Explanation**: The coordination compound contained so many hydroxyls. The acceptor of the hydrogen on the O-H couldn't be located because there was no proper atom such as O or N for the hydroxyl to form hydrogen bond in the radius of 3.6 Å.

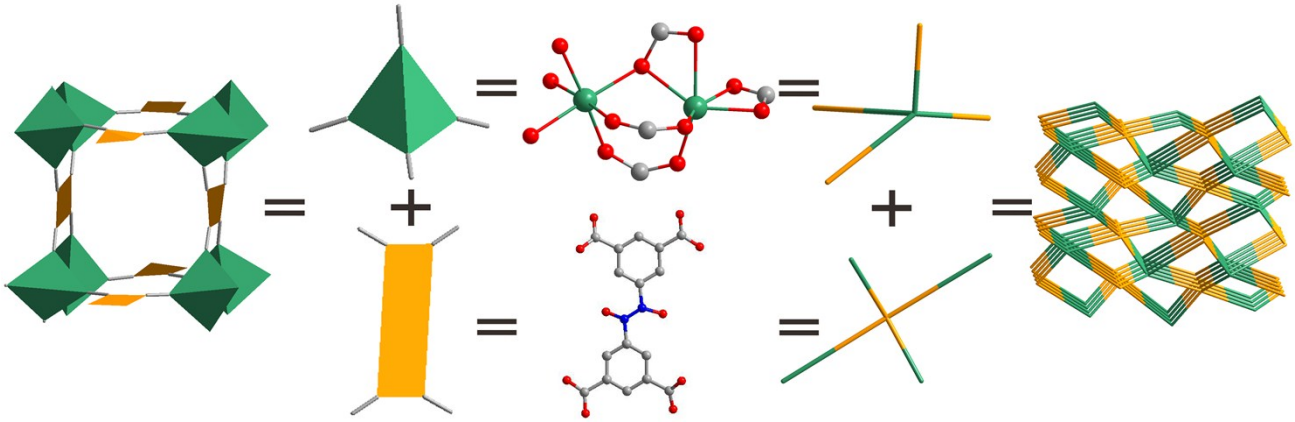

**Fig. S1** A schematic view of the (4, 4)-connected net for **PtS**-type topology presented by complex **1**.

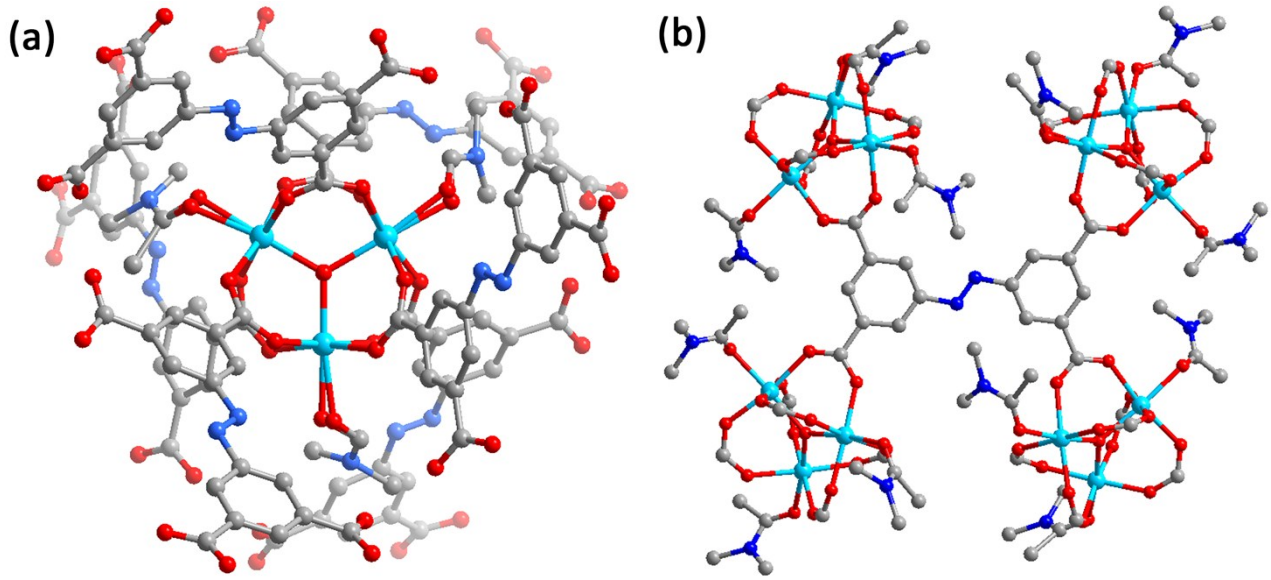


**Fig. S2** (a) The distribution of six $abtc^{4-}$ around each $[Mn_3OH(CO_2)_6]$ SBUs in complex **2**; (b) The distribution of four $[Mn_3OH(CO_2)_6]$ SBUs around each $abtc^{4-}$ in complex **2**.

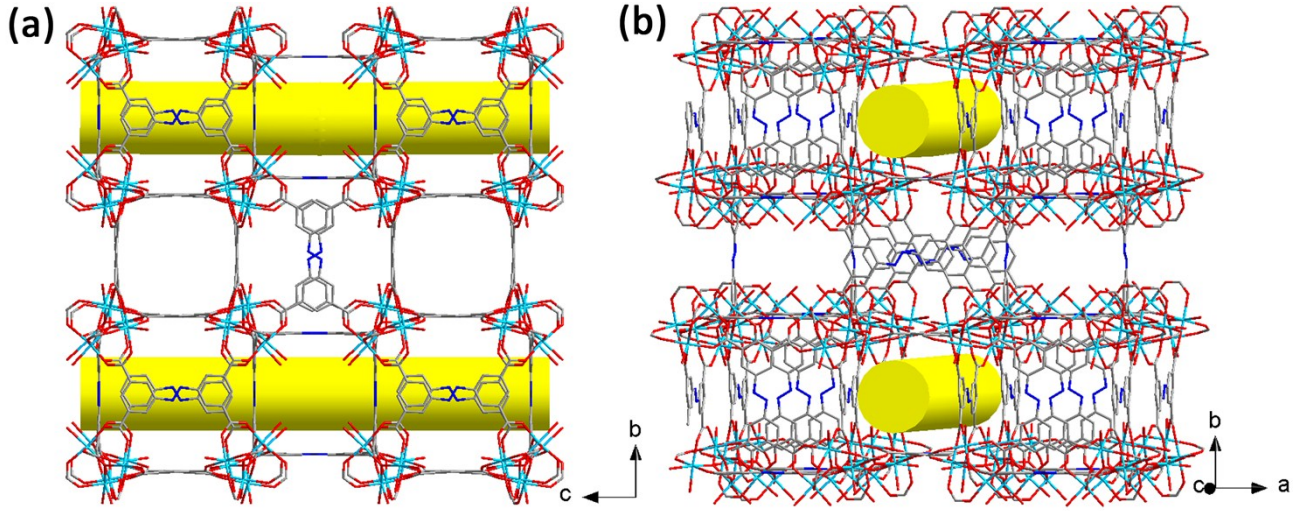


**Fig. S3** The larger channel between the cubic cages along *a*-axis (a) and *c*-axis (b) in complex **2**. $[Mn(H_2O)4]^{2+}$, H atoms, coordinating DMA and $H_2O$ molecules, and free solvent molecules have been omitted for clarity.

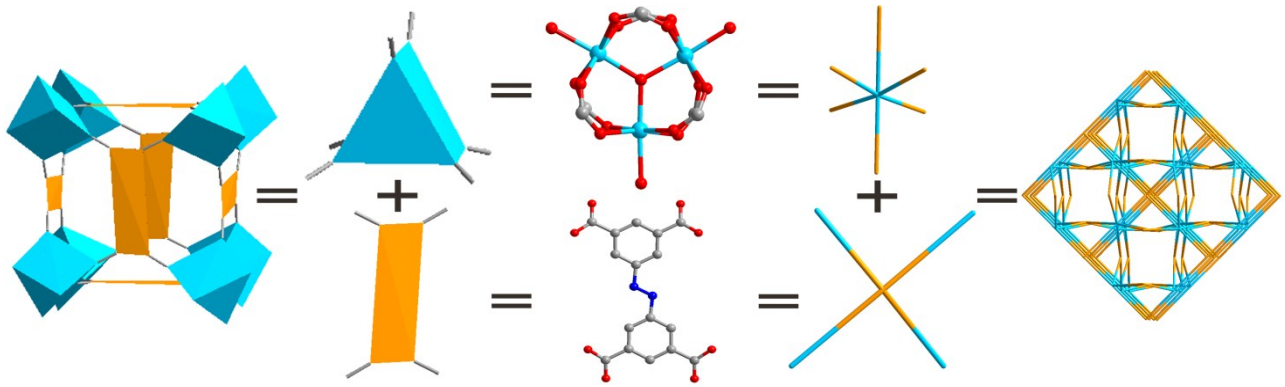

**Fig. S4** A schematic view of the (4,6)-connected net for **soc**-type topology presented by complex **2**.

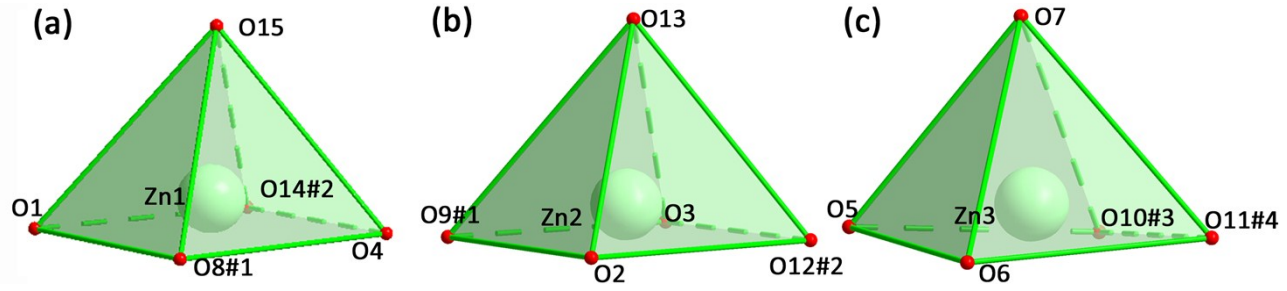


**Fig. S5** The coordination environments of Zn ions in complex **3**. Symmetry code: #1: -x+y, -x, z; #2: 1-x+y, 1-x, z; #3: x-y, 1-y, 1-z; #4: -x+y, 1-x, z.

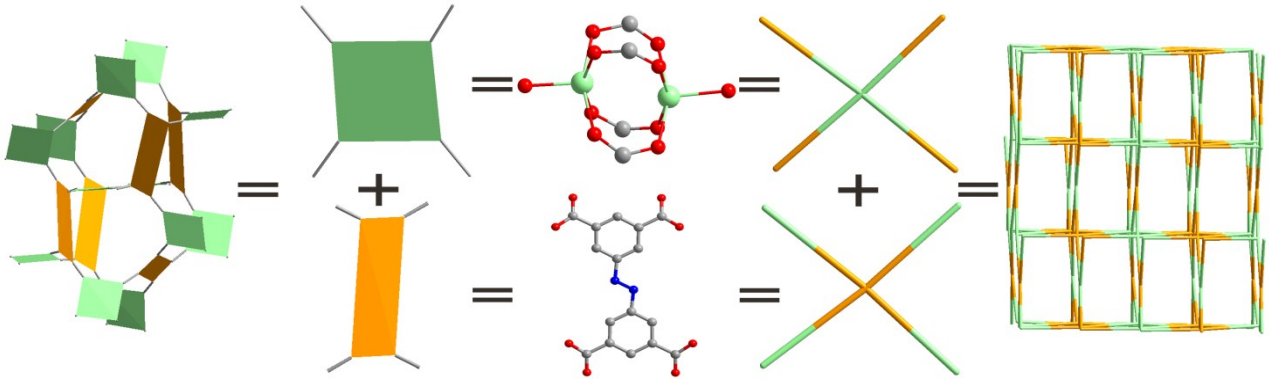

**Fig. S6** A schematic view of the (4,4)-connected net for **NbO**-type topolopy presented by complex **3**.

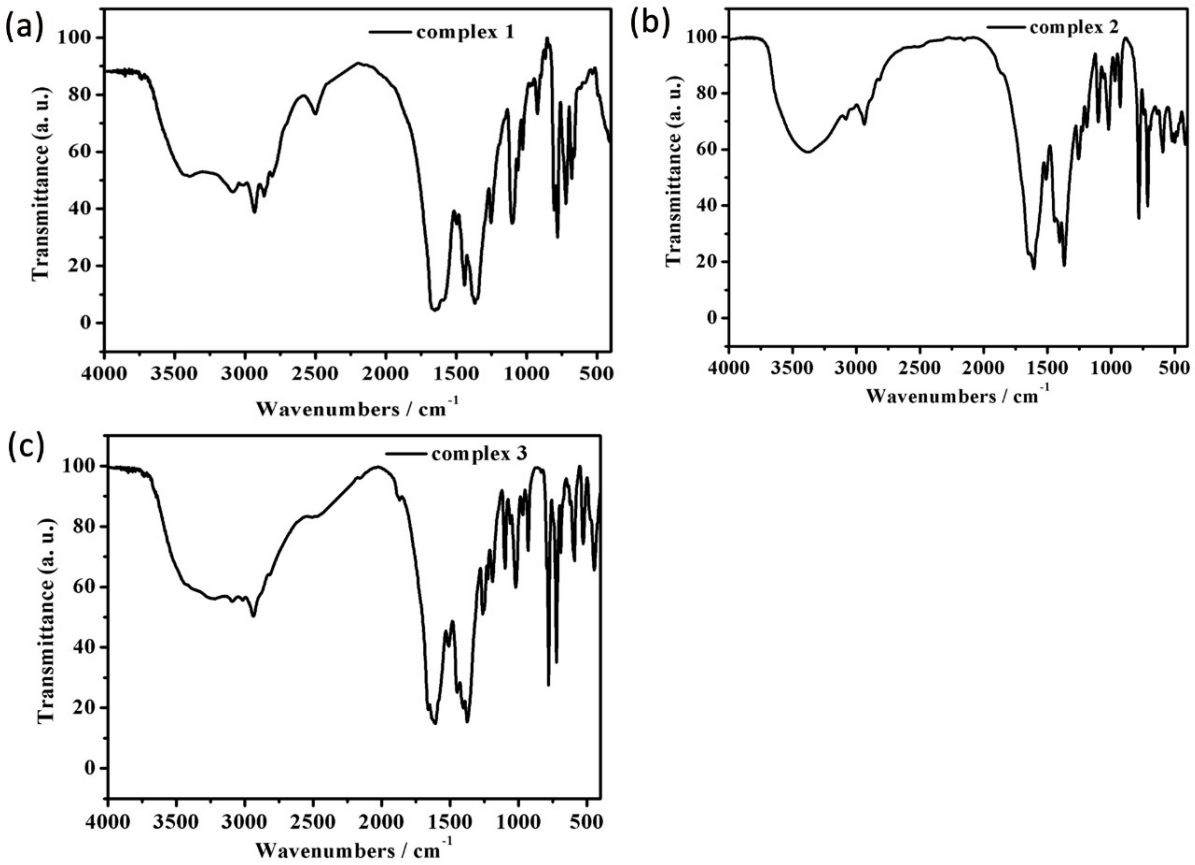


**Fig. S7** IR spectra of **1** a), **2** b), **3** c).

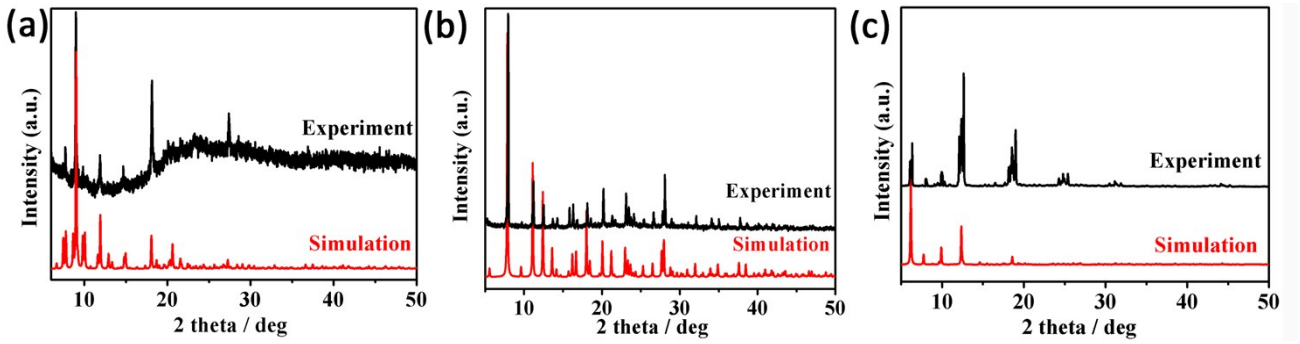


**Fig. S8** Comparison of the simulated and experimental PXRD patterns: **1** a), **2** b), **3** c).

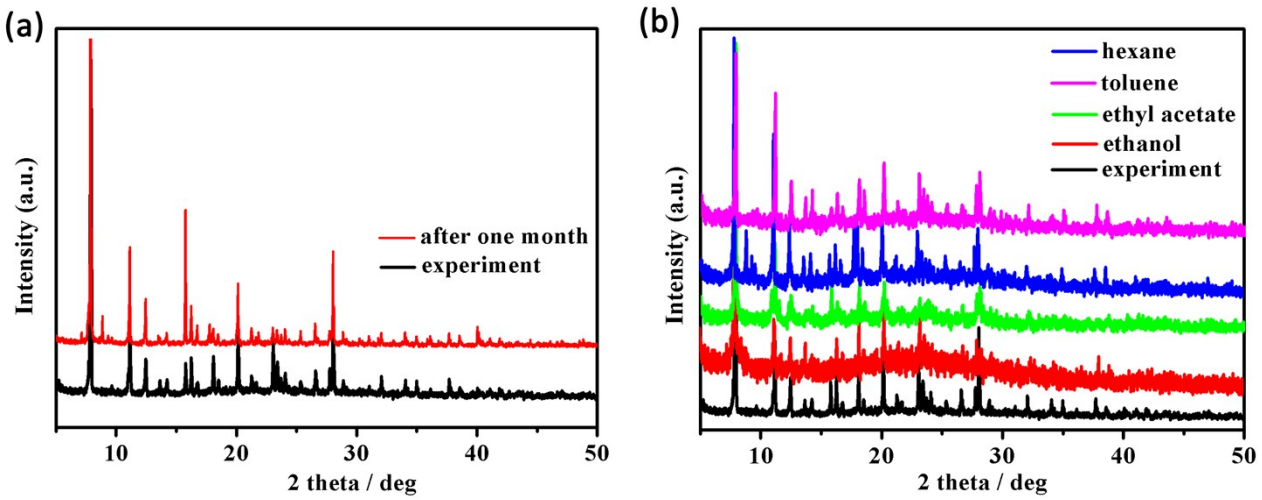


**Fig. S9** (a) Power XRD profiles of **2** after exposing to the air for a month; (b) Power XRD profiles of **2** after being soaked in various boiling solvents for 12 h.

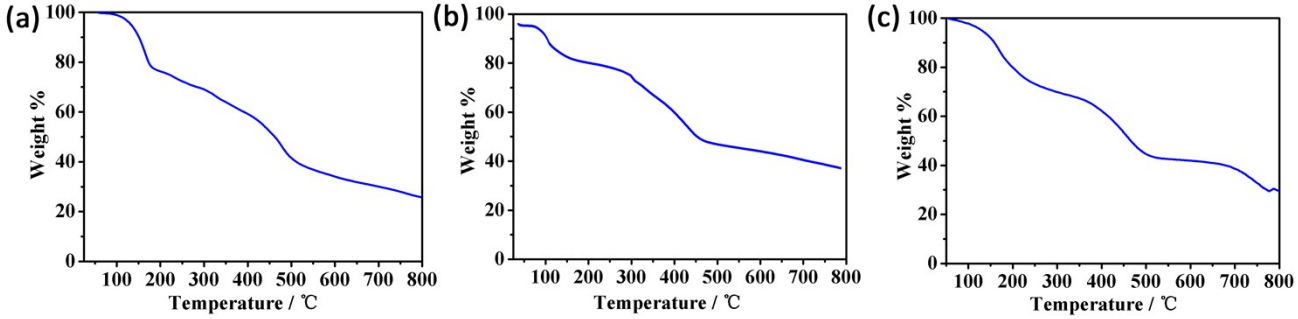


**Fig. S10** The TG curves of **1** a), **2** b), **3** c) on crystalline samples under the $N_2$ atmosphere in the range of 55–800 ˚C.

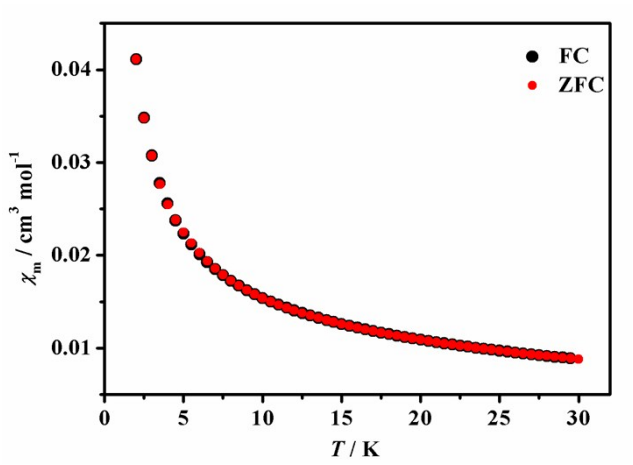


**Figure S11.** The ZFC and FC curves at 50 Oe of **2**.

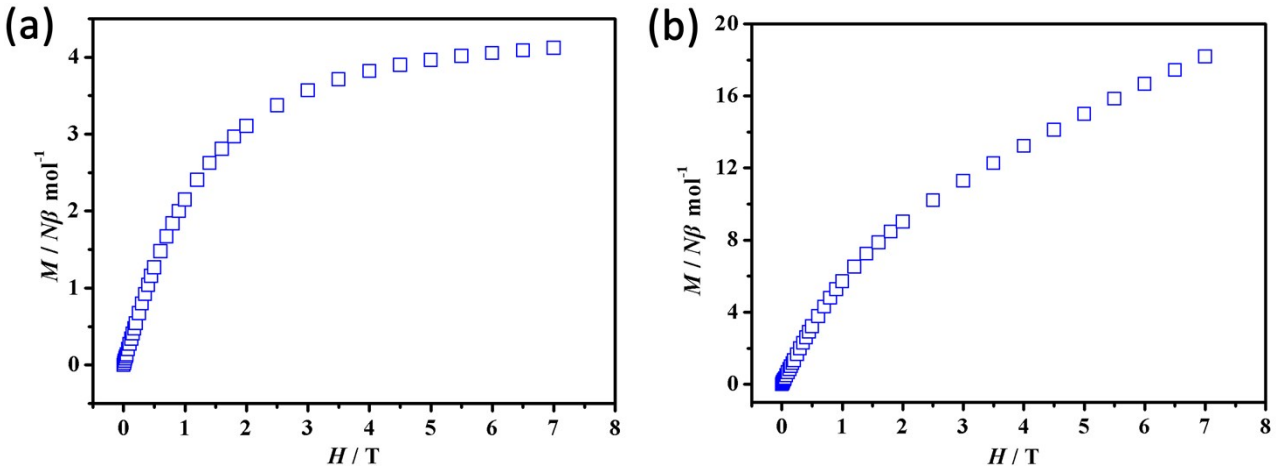


**Fig. S12** Plot of *M*/N*β* vs. *H* at 2 K for complexes **1** a), **2** b).

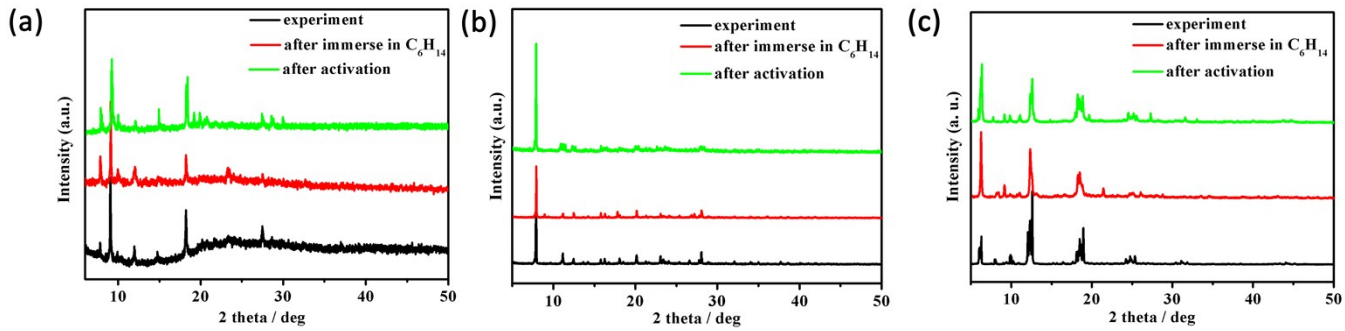


**Fig. S13** Comparison of the experimental and activated PXRD patterns of **1** a), **2** a), **3** b).

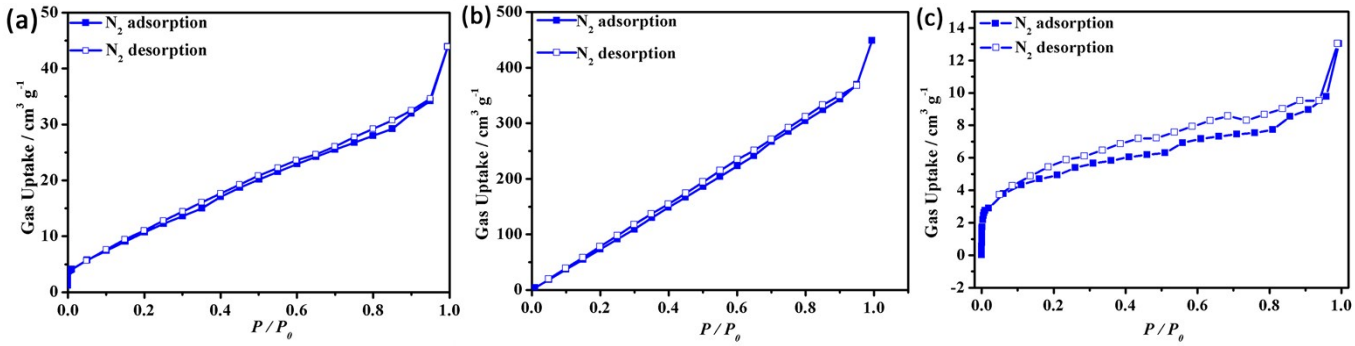


**Fig. S14** Nitrogen sorption isotherm on **1** a), **2** a), **3** b) at 77 K.

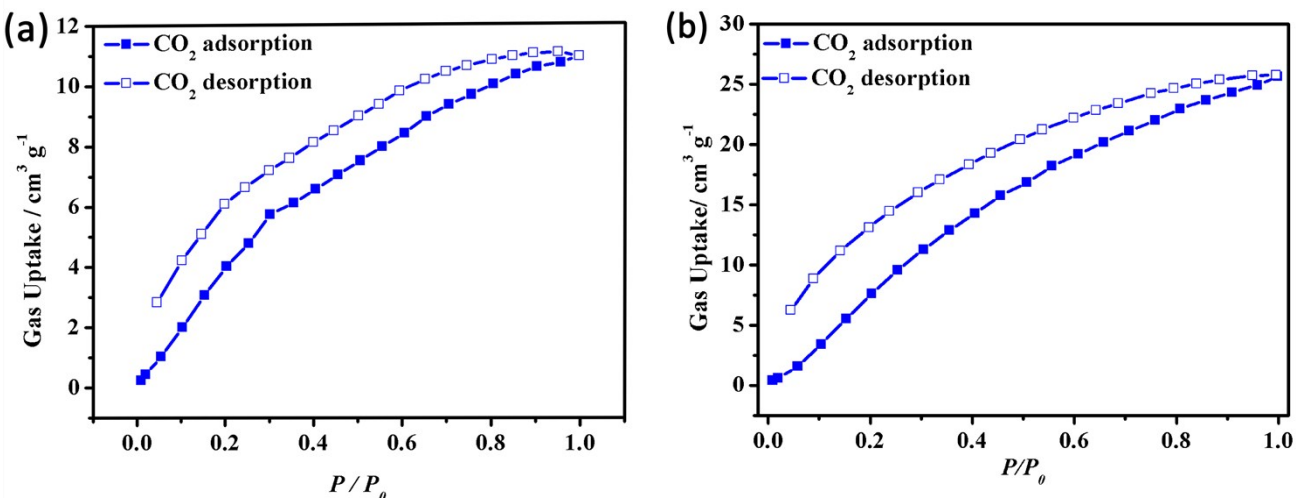


**Fig. S15** Carbon dioxide sorption isotherm on **1** a), **3** b) at 273 K.

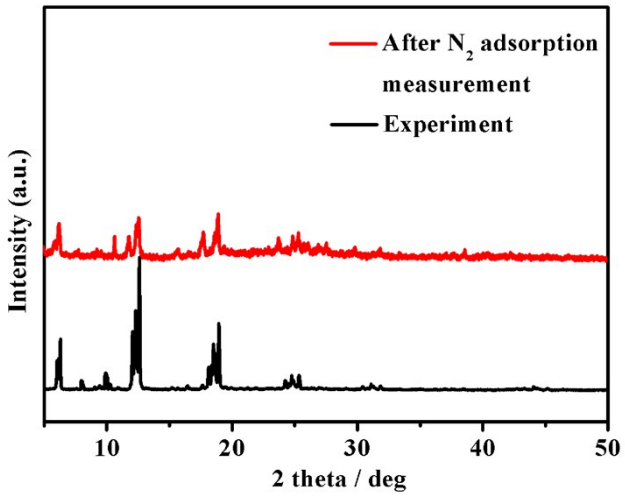


**Fig. S16** The PXRD patterns of the experimental and after $N_2$ adsorption measurement of **3** .

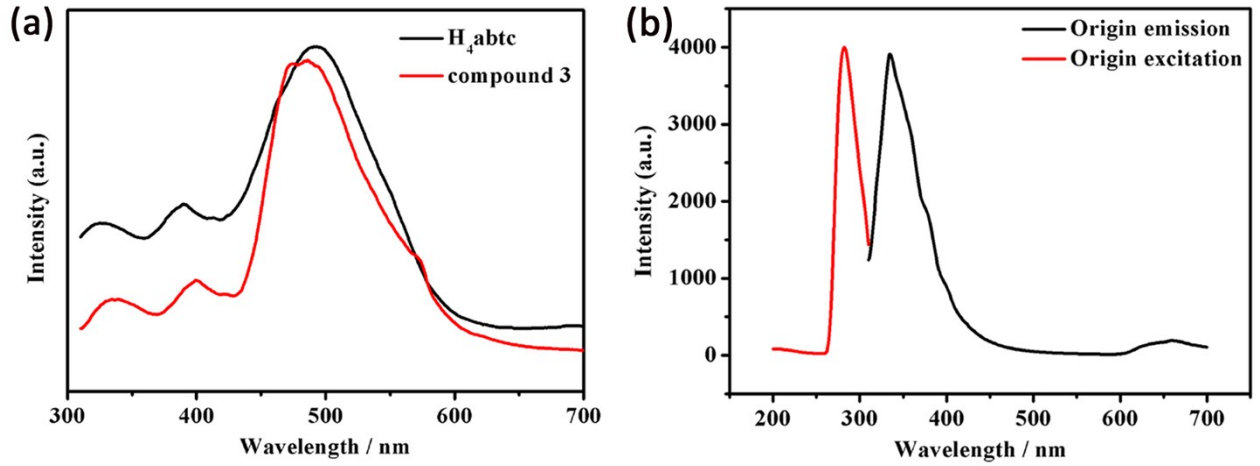


**Fig. S17** (a) Solid-state emission spectrum of $H_4$abtc and **3** at room temperature; (b) The excitation (red) and PL spectra (black) of the origin DMF solution of compound **3**, monitored and excited at 335 nm and 282 nm, respectively

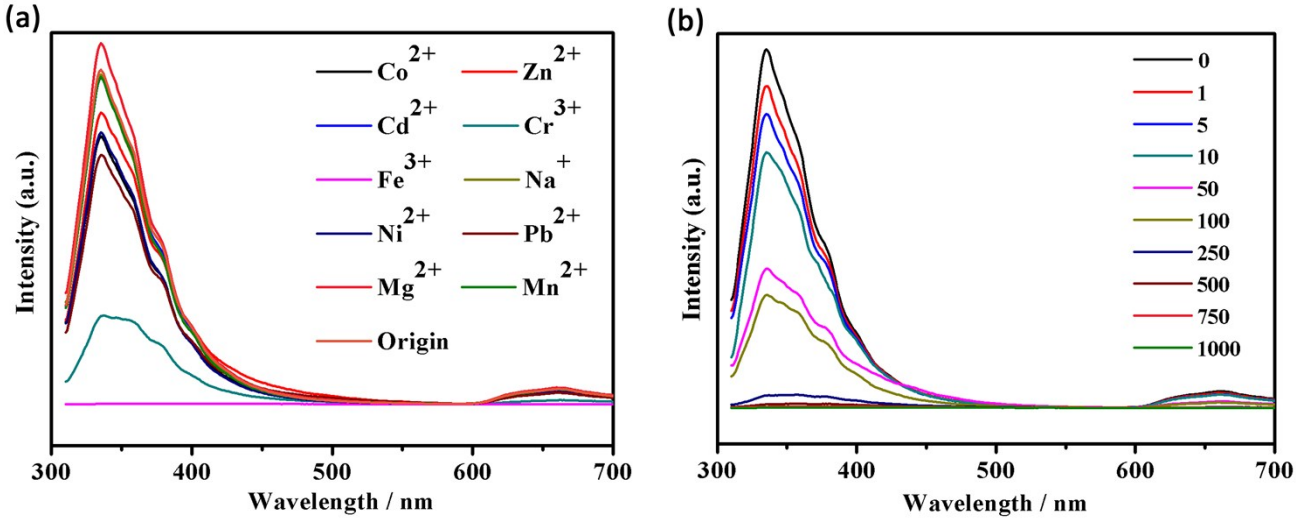


**Fig. S18** (a) Luminescence spectra and of the DMF suspensions of complex **3** with the different metal ions; (b) Luminescence spectra of suspensions the DMF suspensions of complex **3** after adding different volume of $Fe^{3+}$ ions solutions.

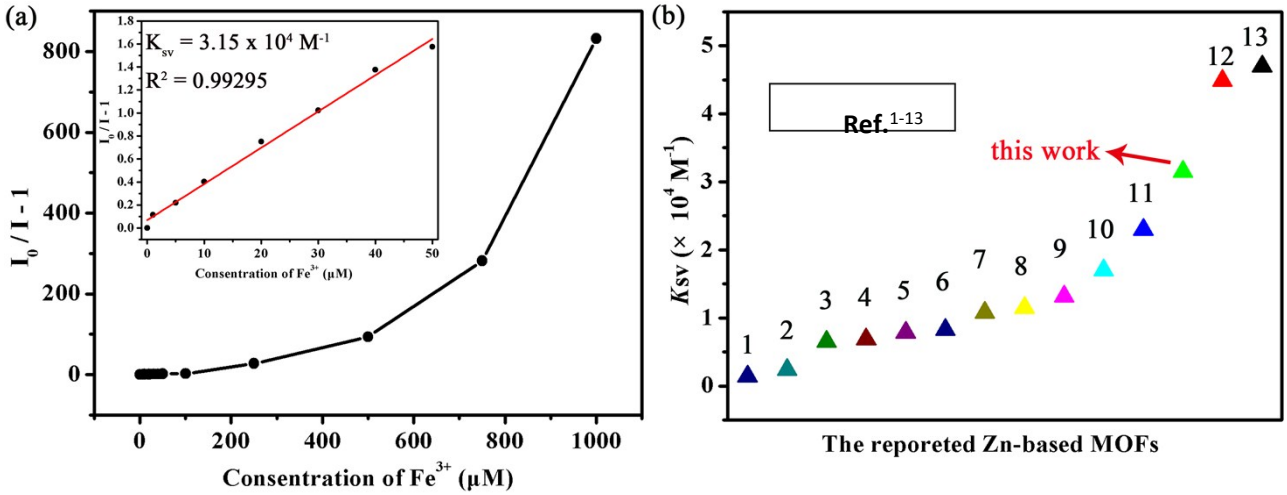


**Fig. S19** (a) Stern−Volmer plot of $I_0/I$ versus $Fe^{3+}$ concentration in DMF suspension for **3** (inset: the linear relationship between $I_0/I$ and low concentration of $Fe^{3+}$ ions). (b) The comparison of $K_{sv}$ values between Zn-based MOFs reported and our work for sensing $Fe^{3+}$ ions.

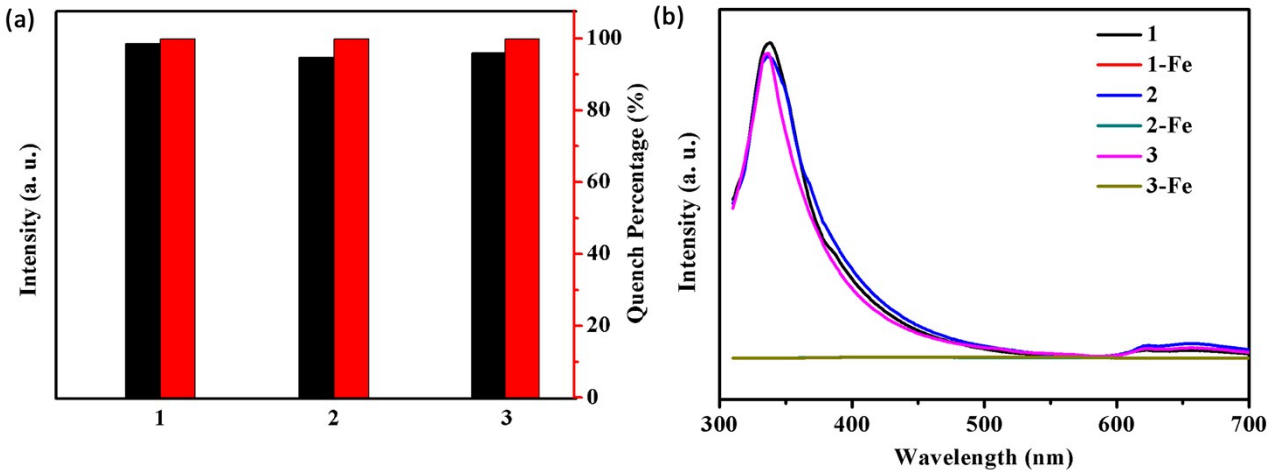


**Fig. S20** (a) Recycle tests of complex **3** by the monitoring of the luminescence intensity at 335 nm and the luminescence quenching percentage before (black) and after (red) adding of $Fe^{3+}$ ions (1 mmol $L^{-1}$). (b) Luminescence spectra of suspensions the DMF suspensions of complex **3** after adding 1mmol $L^{-1}$ $Fe^{3+}$ ions solutions from the first to third cycles in the recycle tests.

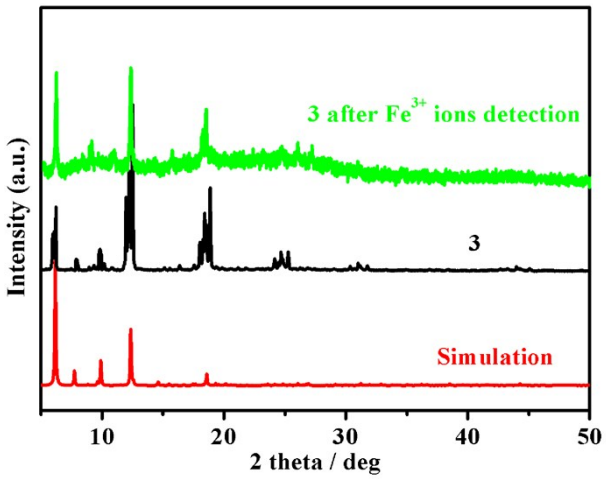


**Fig. S21** PXRD patterns of simulated and complex **3** before and after three cycles toward the detection of $Fe^{3+}$ ions.

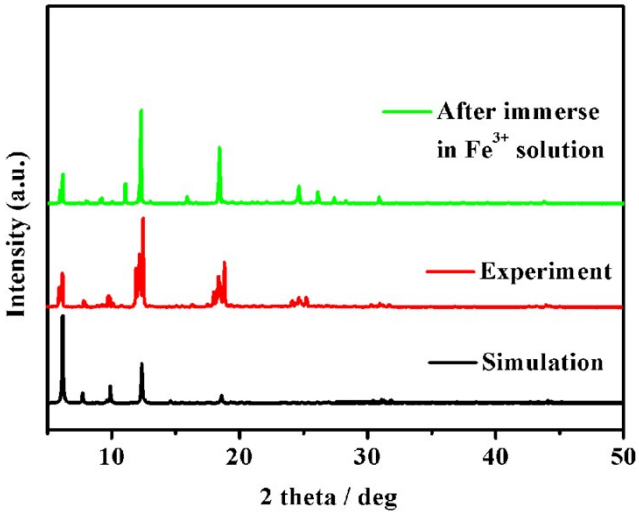


**Fig. S22** The patterns simulated for compound **3**, and PXRD patterns of compound **3** as-synthesized and immersed in $Fe^{3+}$ DMF solution at room temperature.

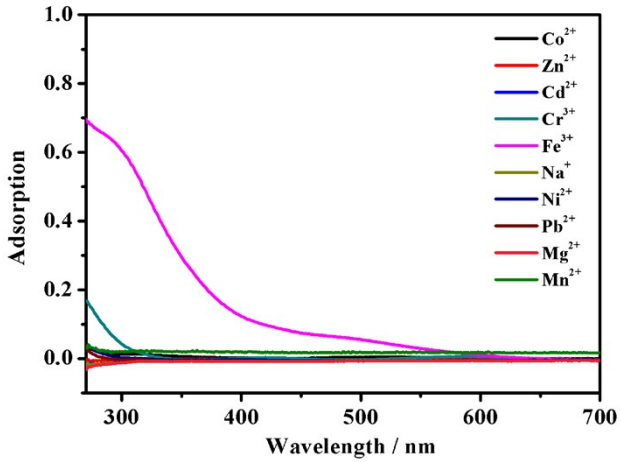


**Fig. S23** UV-Vis spectra of different metal ions with the same concentration (0.2 mmol $L^{-1}$).

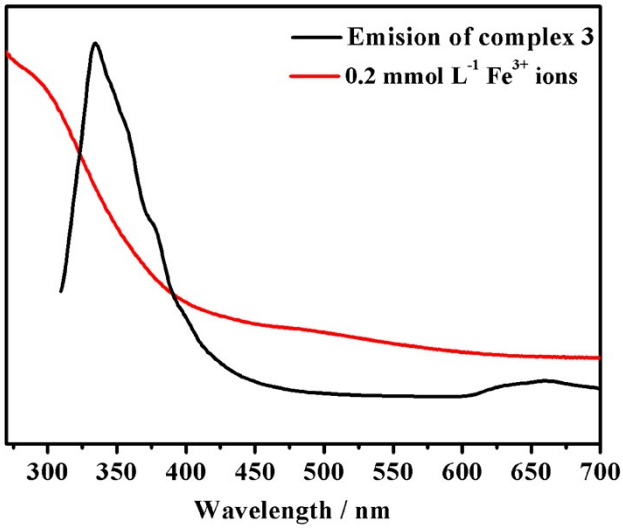


**Fig. S24** UV-Vis spectra of $Fe^{3+}$ ions DMF solutions (0.2 mmol $L^{-1}$) and emission spectrum of complex **3**.

## References


1. P. Hao, Q. Huang, L. Gu, Y.-H. Yu and D.-S. Ma, *Polyhedron*, 2018, **149**, 117-125.
2. F. L. Hu, Y. X. Shi, H. H. Chen and J. P. Lang, *Dalton Trans.*, 2015, **44**, 18795-18803.
3. Y. Q. Zhang, V. A. Blatov, T. R. Zheng, C. H. Yang, L. L. Qian, K. Li, B. L. Li and B. Wu, *Dalton Trans.*, 2018, **47**, 6189-6198.
4. M. Arici, *Cryst. Growth Des.*, 2017, **17**, 5499-5505.
5. J.-C. Jin, J. Wu, Y.-X. He, B.-H. Li, J.-Q. Liu, R. Prasad, A. Kumar and S. R. Batten, *CrystEngComm.*, 2017, **19**, 6464-6472.
6. C. H. Chen, X. S. Wang, L. Li, Y. B. Huang and R. Cao, *Dalton Trans.*, 2018, **47**, 3452-3458.
7. Y. Jiang, L. Sun, J. Du, Y. Liu, H. Shi, Z. Liang and J. Li, *Cryst. Growth Des.*, 2017, **17**, 2090-2096.
8. M.-Y. Sun and D.-M. Chen, *Polyhedron*, 2018, **147**, 80-85.
9. Z. J. Wang, F. Y. Ge, G. H. Sun and H. G. Zheng, *Dalton Trans.*, 2018, **47**, 8257-8263.
10. Z. F. Wu and X. Y. Huang, *Dalton Trans.*, 2017, **46**, 12597-12604.
11. J.-L. Du, X.-Y. Zhang, C.-P. Li, J.-P. Gao, J.-X. Hou, X. Jing, Y.-J. Mu and L.-J. Li, *Sensors and Actuators B*, 2018, **257**, 207-213.
12. J.-C. Jin, X.-R. Wu, Z.-D. Luo, F.-Y. Deng, J.-Q. Liu, A. Singh and A. Kumar, *CrystEngComm.*, 2017, **19**, 4368-4377.
13. Y. T. Yan, W. Y. Zhang, F. Zhang, F. Cao, R. F. Yang, Y. Y. Wang and L. Hou, *Dalton Trans.*, 2018, **47**, 1682-1692.